BJR

HIP

Effect of femoral canal shape on mechanical stress distribution and adaptive bone remodelling around a cementless tapered-wedge stem

M. Oba,
Y. Inaba,
N. Kobayashi,
H. Ike,
T. Tezuka,
T. Saito

Yokohama City University, Japan

Objectives

In total hip arthroplasty (THA), the cementless, tapered-wedge stem design contributes to achieving initial stability and providing optimal load transfer in the proximal femur. However, loading conditions on the femur following THA are also influenced by femoral structure. Therefore, we determined the effects of tapered-wedge stems on the load distribution of the femur using subject-specific finite element models of femurs with various canal shapes.

Patients and Methods

We studied 20 femurs, including seven champagne flute-type femurs, five stovepipe-type femurs, and eight intermediate-type femurs, in patients who had undergone cementless THA using the Accolade TMZF stem at our institution. Subject–specific finite element (FE) models of pre- and post-operative femurs with stems were constructed and used to perform FE analyses (FEAs) to simulate single-leg stance. FEA predictions were compared with changes in bone mineral density (BMD) measured for each patient during the first post-operative year.

Results

Stovepipe models implanted with large-size stems had significantly lower equivalent stress on the proximal-medial area of the femur compared with champagne-flute and intermediate models, with a significant loss of BMD in the corresponding area at one year post-operatively.

Conclusions

The stovepipe femurs required a large-size stem to obtain an optimal fit of the stem. The FEA result and post-operative BMD change of the femur suggest that the combination of a large-size Accolade TMZF stem and stovepipe femur may be associated with proximal stress shielding.

Cite this article: *Bone Joint Res* 2016;5:362–369

Keywords: Tapered-wedge stem; Finite element analysis; Total hip arthroplasty; Adaptive bone remodelling

Article focus

- The aim of our study was to explore the effect of femoral canal shape on the distribution of mechanical stress in the proximal and distal femur after total hip arthroplasty using a cementless tapered-wedge stem.
- We hypothesised that a mismatch between femoral canal shape and stem size would alter the distribution of mechanical stress, resulting in localised stress shielding on the femur.

Key messages

- Using finite element modelling and simulation, the median predicted mechanical stress in the proximal femur was comparatively low for femurs with a stovepipe canal implanted with a large-size stem.
- Results of finite element analysis were confirmed by Dual-energy X-ray absorptiometry analysis, with a loss in bone mineral density in the proximal region of the femur in patients with a stovepipe canal implanted with a large-size stem.

M. Oba, MD,
Y. Inaba, MD, PhD,
N. Kobayashi, MD, PhD,
H. Ike, MD, PhD,
T. Tezuka, MD, PhD,
T. Saito, MD, PhD,
Department of Orthopaedic Surgery, Yokohama City University, s3-9, Fukuura, Kanazawa-ku, Yokohama-city, Kanagawa, 236-0004, Japan.

Correspondence should be sent to Dr Y. Inaba;
e-mail: yute0131@med.yokohama-cu.ac.jp

doi:10.1302/2046-3758.59.2000525

Bone Joint Res 2016;5:362–369.
Received: 17 September 2015;
Accepted: 23 June 2016

Strengths and limitations

- Strength: Construction of patient-specific finite element models based on post-operative CT images for realistic simulation of the interaction between femur structure and stem size and position.
- Limitations: Assumption of a fully bonded stem and simplification of the bone-stem interface condition in the finite element analysis, and a relatively small number of patients.

Introduction

Total hip arthroplasty (THA), using cementless tapered-wedge femoral stems, has been shown to yield excellent long-term results.[1] Tapered-wedge femoral stems are wedge-shaped in the medial–lateral plane to allow press-fit fixation in the proximal metaphyseal canal of the femur, which is essential to achieve initial stability and optimise mechanical loading on the femur, thereby lowering the risk of proximal stress shielding and periprosthetic bone loss.[2] However, the distribution of mechanical loads within the femur after THA will also be influenced by the structure of a patient's femur.[3] Several authors have reported unfavourable outcomes related to the use of Accolade TMZF cementless tapered-wedge stems (Stryker Orthopedics, Mahwah, New Jersey), with a mismatch between the size of the stem and the shape of the proximal femoral canal being associated with post-operative failure.[4,5] As the incidence of post-operative failure of THA is relatively rare, it is presumed in practice that a good initial fixation can be achieved using an Accolade TMZF stem despite some degree of stem-to-canal mismatch. In addition, it is not clear whether the optimal proximal loading profile of the Accolade TMZF stem would be preserved in these cases. Therefore, the purpose of our study was to investigate the mechanical load distribution on the proximal femur after THA using an Accolade TMZF stem with various canal shapes, using finite element (FE) modelling and finite element analysis (FEA).[6]

We chose to construct patient-specific FE models of the post-operative femur with implant *in situ*, rather than use standardised models of the femur, in order to achieve a more realistic assessment of the load distribution for different femur shapes. FE models were constructed from post-operative computed tomography (CT) images, the model thereby reflecting the original femoral structure and stem position in real subjects. We focused on the relative percentage change in the calculated strain energy density (SED) and von Mises stress (VMS) between pre- and post-operative femur models in our FEA results for mechanical stimuli on bone remodelling in post-operative femurs. This approach of correlating FEA-estimated load distribution and changes in periprosthetic bone mineral density (BMD) after THA has been applied previously.[7-10] Thus, we assumed that our FE simulations could be validated by comparison with these previously reported BMD results.

Patients and Methods

This study was approved by the Institutional Review Board of our institution (B090507020) and all participants provided informed consent. We included 20 patients who underwent THA for dysplastic arthritis of the hip (DDH) using the Accolade TMZF stem at our institution between 1 December 2008 and 31 May 2012. We did this after reviewing the pre-operative anteroposterior radiographs of the hip from 90 consecutive female patients who had undergone primary THA for hip osteoarthritis due to DDH using the Accolade TMZF stem during the same period. Applying the guidelines of Engh, Massin and Suthers,[11] no radiographic evidence of stem implant instability was identified in the study group over the first post-operative year. The width of the proximal femoral canal on the operated side was measured from pre-operative anteroposterior radiographs of the hip, with Noble's canal flare index (CFI) calculated for each patient.[12] Based on Noble's classification, femurs were divided into three groups of femoral canal shapes: champagne flute (CFI ≥ 4.7), intermediate (CFI 3–4.7), and stovepipe (CFI < 3). The distribution of femur canal types among the 20 patients in our study group was as follows: seven patients with a champagne flute-type; five with stovepipe type; and eight femurs which were randomly selected from the remaining 78 femurs with intermediate canal type to balance the groups for analysis. Relevant demographics of our study group are listed in Table I. All 20 femurs included in the analysis were from female patients, with a median age of 62 years (49 to 76). Stem alignment was determined from the post-operative anteroposterior radiographs of these femurs by measuring the angle between the long axis of the femur and the stem. We defined stem alignment of less than 2º with respect to the femoral long axis as neutral.[13]

FE modeling and FEAs were performed using Mechanical Finder (MF, version 6.2; RCCM Inc., Shinagawa, Tokyo, Japan), an all-in-one software package that includes a 3D modeler, meshing component, and FE solver.[6,9,10] Patient-specific FE models of femurs were constructed from CT images, 2 mm slice thickness, obtained pre-operatively and one week post-surgery using a Sensation 16 scanner (Siemens AG, Erlangen, Germany), with a tube voltage and current of 140 kV and 300 mA, respectively. Scanned images from the proximal two thirds of the entire femur were used for FE modeling. The CT image datasets were segmented using the global threshold algorithm function of the MF software,[6] with a threshold of 300 Hounsfield units (HU) for the bone area and 3000 HU for the stem. Manual correction of the segmentation was performed as necessary. Subsequently, the segmented image datasets of the pre- and post-operative femur and stem were converted to 3D models and

Table I. Relevant demographics of the study group

	Champagne flute	Intermediate	Stovepipe
Patients (n)	7	8	5
Age (yrs)*	62.0 (53 to 63)	62.5 (62 to 75)	58.0 (56 to 66)
BMI*	22.7 (22.0 to 27.0)	23.9 (19.4 to 27.9)	20.0 (19.0 to 22.4.2)
CFI*	5.0 (4.9 to 5.4)	3.8 (3.4 to 4.2)	2.7 (2.6 to 2.7)
Height*	152.0 (151.0 to 155.0)	153.0 (149.0 to 155.0)	157.7(157.0 to 161.0)
Pre-operative bone quality			
BMD of proximal femur (g/cm^2)*			
Proximal (zone1 + zone7)	0.76(0.62to 0.96)	0.8(0.72 to 0.9)	0.7(0.67 to 0.71)
Middle (zone2 + zone6)	1.25(0.92 to 1.34)	1.13(1.01 to 1.19)	1.14(0.9 9to 1.19)
Distal (zone3 + zone 5)	1.57(1.36 to 1.70)	1.46(1.39 to 1.55)	1.32(1.29 to 1.53)
Pre-operative lumbar T-score (L2 to L4)*	-0.2 (-0.2 to 0.3)	-1.8 (-2.3 to 0.1)	-2.2 (-3.0 to -1.9)
Stem size*	2.0 (1.8 to 2.5)	3.0 (2.9 to 3.2)	3.5 (3 to 4)

*Values are expressed as the median (IQR)

BMI, body mass index; CFI, canal flare index; BMD, bone mineral density

T-score represents the number of standard deviations from the mean bone mineral density in young adult population of the same gender

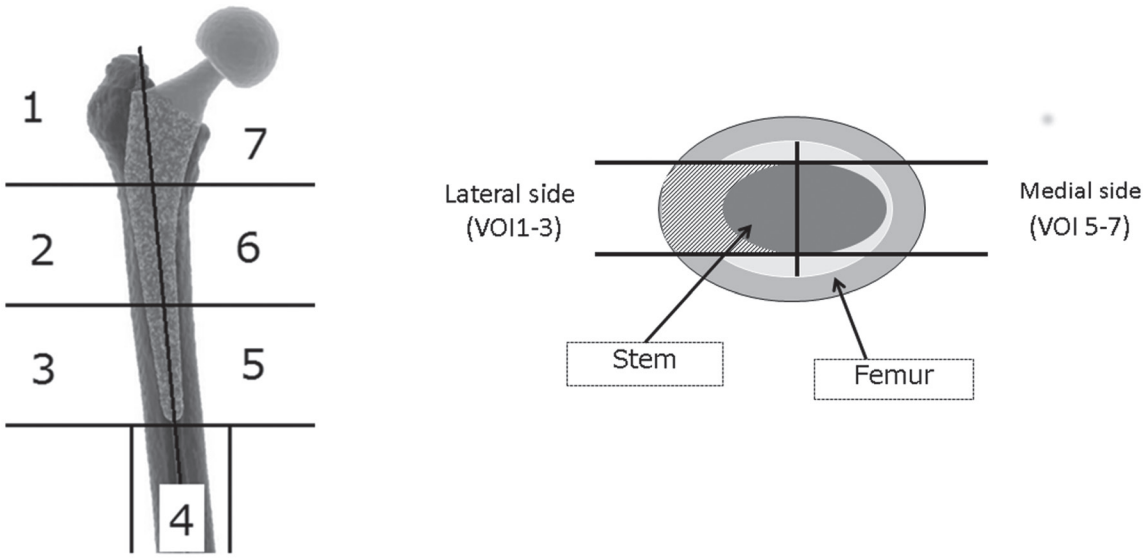

Fig. 1

Segmentation of the finite element models of the femur (a) in the coronal plane according to Gruen's zones,[14] and (b) in the horizontal plane to create seven volumes of interest (VOIs).

meshed. To evaluate mesh convergence, we constructed models with nine levels of mesh refinement from a CT dataset of one representative case from the intermediate group, and performed FE analyses with the same boundary conditions, as described in the following section. The mean value of SED and VMS in the proximal femur (volumes of interest (VOI) 1, 2, 6, and 7; Fig. 1a)[14] was considered to be the indicator of convergence. The percentage changes in the mean value of the two indicators between the 1.5 mm to 2 mm mesh model and the 2 mm to 4 mm mesh model were 1.2% (VMS) and 0.4% (SED). The percentage changes in these values between the 2 mm to 4 mm mesh model and 2.5 mm to 3 mm mesh model were 6.9% (VMS) and 6.2% (SED) (Fig. 2). In accordance with the results of the mesh convergence test, the mesh size of each element was set to 2 m to 4 mm for our femur models. The approximate number of elements for the pre-operative femur model, post-operative femur model, and stem were 100 000, 101 000 and 40 000, respectively. The material property (Young's modulus) of each element was calculated from the CT number (HU) of the pixel at the same location of the element. If the element possessed multiple pixels on CT images, the mean CT number of pixels within the element was calculated. To reduce the sampling error when calculating the mean value of the element, we set multiple (17) sampling points within each element using the MF version 7.0 software to reduce the effects of noise and partial volume when the average CT number of the element was calculated. We calculated the apparent density (ρ in g/cm^3) of each element according to the CT number of the element using Equation 1 (Table II). Next, we calculated the elastic modulus (E (MPa)) of each element from the apparent density (ρ) value using Equation 2

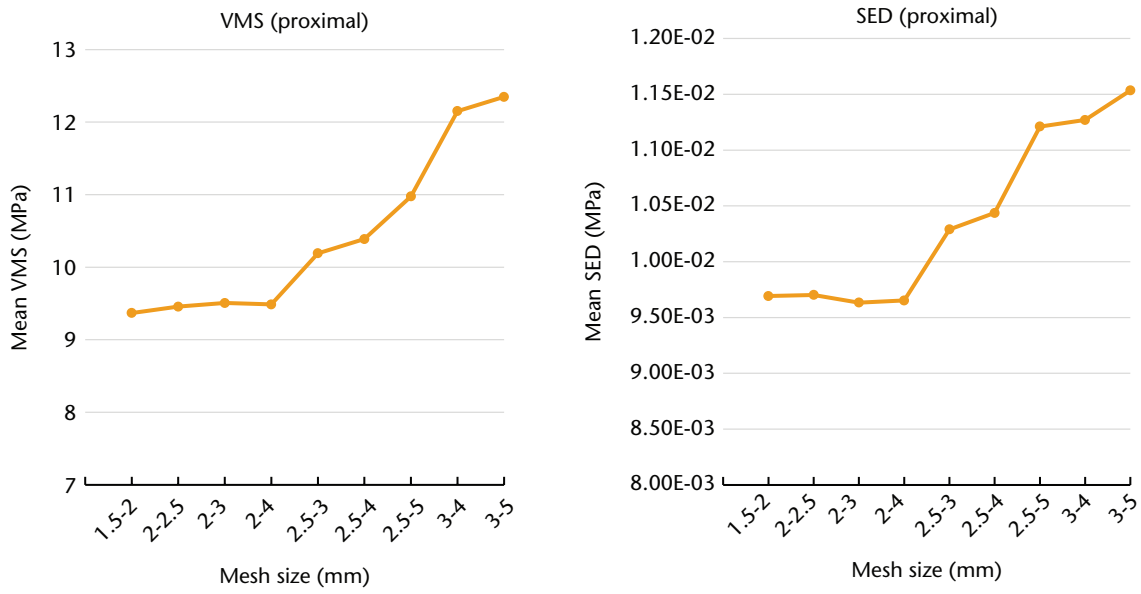

Fig. 2

Results of the mesh convergence test. (VMS: von Mises stress, SED: strain energy density.)

Table II. Equations

Equation 1	
$\rho(g/cm^3) = (HU + 1.4246) \times 0.001/1.058$	(HU > -1)
$\rho(g/cm^3) = 0$	(HU ≤ -1)
Equation 2	
$E = 0.001$	($\rho = 0$)
$E = 33\,900\rho^{2.20}$	($0 < \rho \leq 0.27$)
$E = 5307\rho + 469$	($0.27 < \rho < 0.6$)
$E = 10200\rho^{2.21}$	($\rho \leq 0.6$)

Equation 1, determines apparent bone mineral density (g/cm^3) using Hounsfield's unit (HU); Equation 2, proposed by Keyak,[15] is used to calculate Young's modulus (E) from apparent bone mineral density

(Table II), according to Keyak et al's[15] density–elasticity relationship theory. The Poisson's ratio of the bone was set to 0.40.[15] The Accolade TMZF stem was modeled as a homogeneous and isotropic element, with an elastic modulus of 79.5 GPa and a Poisson's ratio of 0.33.[16] To simulate the stem interface, which was successfully osteointegrated into the femur, we assumed that the stem was completely bonded to the bone in our FEA model. The loading condition simulating simplified single-leg stance was used[7,9,10] to evaluate the distribution of mechanical load. The following inputs were used for the simulation-based FEAs: a joint reactive force of 2400 N exerted by the weight of the body on the femoral head or the prosthetic head at an angle of 15° relative to the femoral axis, and a 1200 N force generated by the abductor muscles exerted at an angle of 20° relative to the greater trochanter. The model was completely clamped at the distal end of the femur.

After linear FEA of the pre- and post-operative femur model was performed, each model was further segmented into seven volumes of interest (VOIs), based on the zones of the femur described by Gruen[14] (Fig. 1) to evaluate the FEA results. We focused on SED[17,18] and VMS[8,19] in our FEA model as parameters of mechanical stimuli on bone remodelling in reference to previous studies. To assess post-operative changes in the VMS and SED distribution, we calculated the relative percentage change of the VMS and SED of the elements within each VOI, with the mean value used as the representative value of that VOI for analysis. The magnitude of percentage change of the VMS and SED between the pre- and post-operative femur models in each VOI was compared among the three femur canal groups.

To quantify the post-operative bone remodelling in the patient's femur, we compared the changes in post-operative femur BMD during the first post-operative year to the results of our FEAs. Changes in femur BMD were assessed by Dual Energy X-ray absorptiometry DEXA (Hologic Discovery device, Hologic Inc., Bedford, Massachusetts); measures obtained at one week post-surgery were used as a baseline reference for comparisons with measures obtained at three months, six months, and one year post-surgery. Scanning of the proximal femur was performed in the anteroposterior plane, with the BMD quantified in the seven zones of Gruen,[16] using the "Array Prosthetic Mode" to avoid including the metal stem in the scanning area. Gruen's zones used in the DEXA measurement corresponded to the VOIs (1 to 7) in the assessment of the FEA results. The BMD measured at each time point was converted to a percentage ratio relative to the baseline BMD measure. Pre-operative BMD data of the femur on the operated side and the second to fourth lumbar vertebrae (L2–L4) were also obtained in

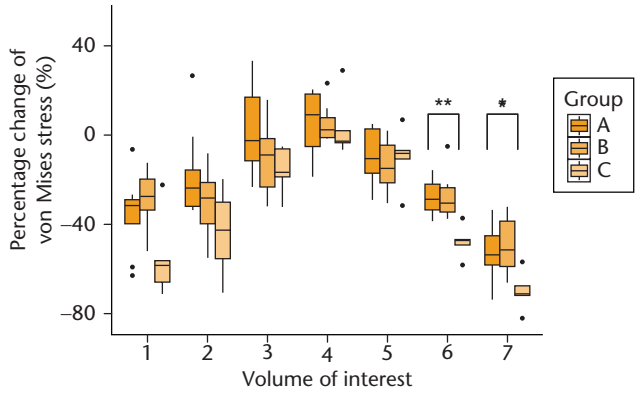

Fig. 3

Comparison of relative percentage change of von Mises stress between pre- and post-operative femur model for the three groups. Post-operative relative percentage change of von Mises stress in each volume of interest compared with that of pre-operative models. Dots in the boxplot show outlier. (*, p = 0.02; **, p = 0.01.)

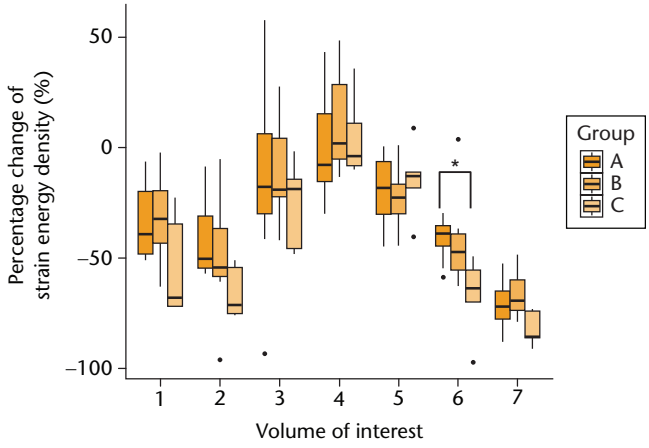

Fig. 4

Comparison of the relative percentage change in the strain energy density between pre-operative and post-operative femur models among the three groups. The post-operative relative percentage change of strain energy density in each volume of interest compared with that of the pre-operative models. Dots in the boxplot represent outliers. (*, p = 0.047; **, p = 0.03.)

the lateral view to determine the presence and extent of osteoporotic tendency for each patient.[20]

Statistical analyses were performed using R software (version 3.0.1; R Foundation for Statistical Computing, Vienna, Austria). Between-group comparisons were evaluated using the Kruskal–Wallis rank-sum test. All numerical data were nonparametric, and they are expressed as medians and interquartile ranges (IQRs) in brackets. Linear regression analysis was performed to examine the relationship between our FEA results (VMS and SED) and the BMD change. A p-value of < 0.05 was considered to be statistically significant, *a priori*.

Results

The selection of stem sizes (Table I) varied among the three groups with a proximal femoral canal shape; larger-size stems were selected for the stovepipe group (median size #3.5, IQR 3 to 4) and smaller-size stems were selected for the champagne-flute group (median size #2, IQR 1.75 to 2.5). Regarding baseline bone quality of the patients (Table I), the median BMD of L2–L4 was relatively lower for patients in the stovepipe group than for patients in the other two groups. BMD of the proximal femur preoperatively showed a slight osteoporotic tendency in the stovepipe group. Stem alignment was 3° valgus in one subject and neutral in 19 subjects.

The mean percentage changes of VMS in each VOI between the pre- and post-operative femur models were calculated from the FEA results, and they are plotted in Figure 3. Between–group differences in the pattern of post-operative change of the VMS were identified, and specific differences were seen in VOIs 6 (p = 0.01) and 7 (p = 0.02). *Post hoc* analysis indicated that the percentage decrease of VMS in VOI 6 was significant (p = 0.01) in the stovepipe group (-47.3%; IQR -49.2 to -46.8) compared with the champagne-flute group (-28.8%; IQR -33.6 to -22.1) and intermediate group (-30.4%; IQR -34.5 to -23.7). The mean percentage decrease of the VMS in VOI 7 was also significant in the stovepipe group (p = 0.03) (-70.9%; IQR -71.6 to -67.5) compared with the champagne-flute group (-53.7%; IQR -58.3 to -45.2) and intermediate group (-51.4%; IQR -58.9 to -38.5). A significant difference in the percentage change of the SED was seen in VOI 6 (p = 0.03) (Fig. 4). The stovepipe group had a significant decrease in the SED in VOI 6 (-63.8%; IQR -70.0 to -55.4) compared with the percentage decrease in the same VOI in the champagne-flute group (-38.8%; IQR -44.6 to -35.5) and intermediate group (-47.2%; IQR -55.5 to -39.1). There was no statistically significant difference in the SED in VOI 7 among the three groups (p = 0.07).

Changes in the BMD of femurs during the first post-operative year are shown in Figure 5. Significant between–group differences in BMD were evident in Gruen's zones 6 (p = 0.01) and 7 (p = 0.04). In zone 6, a marked decrease in BMD was identified only in the stovepipe group during the first post-operative year. Zone 6 BMD was significantly lower (p = 0.01) in the stovepipe group (-14.3%; IQR -16.6 to -13.4) than in the champagne-flute (-1.4%; IQR -6.9 to +6.8) and intermediate groups (+3.6%; IQR -2.3 to +16.7). A comparable post-operative decrease in BMD in zone 7 was evident in all the groups during the first post-operative year (champagne-flute group -23.1%; IQR -26.8 to -13.5; intermediate group -22.7%; IQR -28.3 to -18.8; stovepipe group -36.5%; IQR -37.8 to -30.6). Additionally, BMD in zone 7 was significantly decreased in the stovepipe group (p = 0.045) compared with the other two groups. BMD values in zones 1 and 2 were lowest in the stovepipe group among three groups during the first post-operative year; however, the difference was not statistically significant.

The percentage change of VMS and SED in each VOI was positively correlated with the post-operative BMD change in the corresponding zone (Fig. 6). A statistically

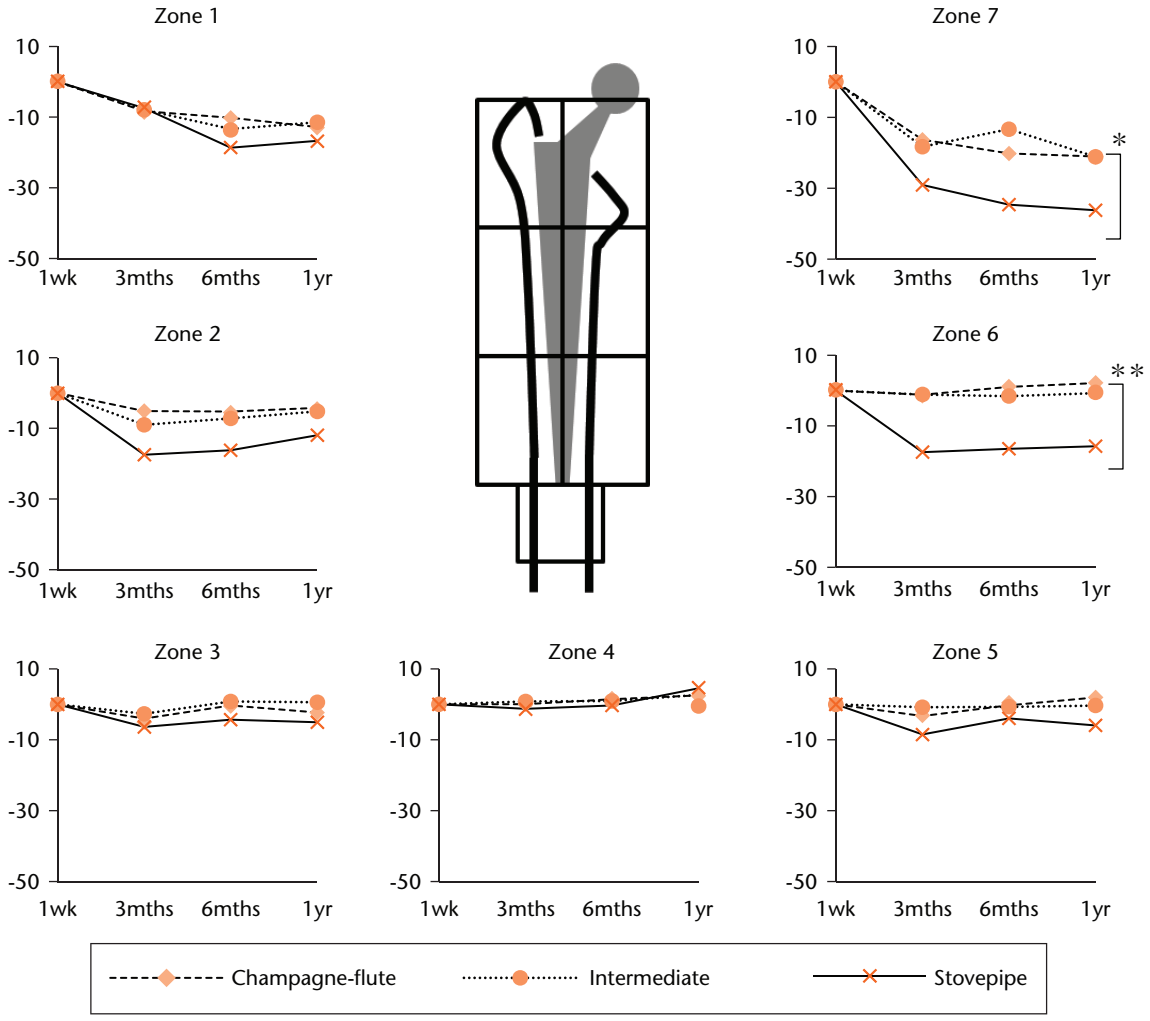

Fig. 5

The median percentage change in bone mineral density after index surgery. The periprosthetic bone mineral density (BMD) at three months, six months, and one year post-surgery is expressed as a percentage change from baseline BMD measured at one week post-surgery. Each Gruen zone corresponds to the volume of interest of the same number from the finite element analysis results. (*, p = 0.04; **, p = 0.01.)

significant correlation was observed between both parameters and the BMD change ($p < 0.01$), and the adjusted R^2 value showed that the percentage change of VMS (adjusted $R^2 = 0.79$) could predict the post-operative BMD change better in our simulation model than the percentage change of SED (adjusted $R^2 = 0.69$).

Discussion

In our study, FEA and DEXA were used to evaluate the effect of stem size and proximal femoral canal shape on the distribution of mechanical stress with the femur after cementless THA, an issue of high clinical significance.[8-10,21] We focused on the SED and VMS as mechanical parameters associated with bone remodelling in the results of our FEA, and those results were significantly correlated with post-operative BMD changes of the patients' femur. Our simulation-based outcomes predicted a stronger stress-shielding effect for the stovepipe-femur group compared with other groups. Although the stress-shielding phenomenon on long-term stability of the stem has not yet been proven,[22] it is clinically important to limit the proximal bone loss due to stress shielding, as this is a risk factor for periprosthetic fracture.[23]

Among the numerous factors that affect the loading profile of the femur after cementless THA, the shape characteristic of the large Accolade TMZF may be one of the causes of the strong stress-shielding effect. Among patients in our study group, the average stem size selected for stovepipe femurs was larger than that used in the other groups. Thus, the broad and flat tip of the large Accolade TMZF stem may have led to distal engagement of the stem even in the stovepipe canal and a decrease in stress transfer at the proximal side of the femur. The result of a computational simulation on the stem design performed by Ruben, Fernandes and Folgado[24] also suggests that a broad stem tip directly contacts the diaphyseal cortex and is associated with proximal stress-shielding.

In addition, increased stiffness of the large-size stem may also lead to stress shielding in the proximal part

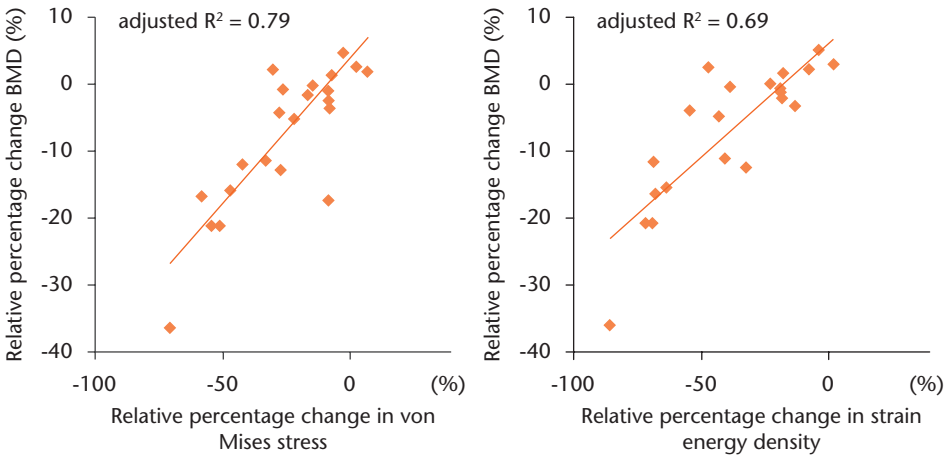

Fig. 6

Scatter plot illustrating the relationship between (a) the percentage change in von Mises stress (VMS) and post-operative bone mineral density (BMD), and (b) the percentage change in strain energy density (SED) and post-operative BMD. Twenty-one points plotted in each scatter plot indicate the mean relative percentage change in the finite element analysis results (VMS or SED) and BMD of each volume of interest (1 to 7) in the three groups. A statistically significant correlation was observed between both parameters and the change in BMD ($p < 0.01$).

of the femur.[25-27] In our study, we constructed a post-operative femur model using post-operative CT data to reflect the implanted stem position and shape. The surgeon decided the size of the implanted stem during pre-operative planning, and selection of the stem size was strongly influenced by the femoral canal shape of each femur. Therefore, we could not assess the magnitude of each factor's contribution independently. Bone remodelling occurs as an adoptive response to mechanical stimulus, therefore, FEA has been used to estimate the magnitude and distribution of mechanical stimulus on the femur after THA in a number of studies.[7-10,16,17-19,21] The strain adoptive theory is a major theory of bone remodelling,[28] and it is assumed that SED calculated in FEA can predict the magnitude of bone remodelling stimulus.[17,18] However, in several studies, the stress parameter could predict bone remodelling better than the strain parameters.[10,29,30] In the present study, the percentage change in VMS correlated better with the post-operative BMD change in the femur after THA than the percentage change in SED. However, further studies will be needed to clarify which parameter can better predict adaptive bone remodelling *in vivo*.

A major limitation of this study was that the interface condition between the stem and the femur in the FEA model was assumed to be fully bonded. The Accolade TMZF has two different surfaces: a proximal hydroxyapatite-coated porous surface and a distal smooth-finished surface. Therefore, different friction coefficients should be set for each surface of the stem to construct a more realistic model. The fully bonded model has been used in several previous studies that focused on the loading conditions of cementless stems,[8-10] which had already been fixed (i.e. osteointegrated) within the femoral canal. According to one study that compared the fully bonded condition and frictional interface condition in an FEA model of a cementless stem,[27] stress analysis of the cementless stem showed a similar result between the two conditions. Although this simplification in FEA may limit the interpretation of our results, we believe that the result of our FEA demonstrates characteristic stress/strain distribution among the three femoral canal groups, assuming that the cementless stem is successfully fixed. Secondly, the relatively small number of patients increased variance of the data and restricted the statistical analyses. We could only include five subjects with stovepipe femurs. With a larger sample size, we may be able to detect other significant differences in our FEA results among the three groups in addition to those already mentioned. However, the incidence of stovepipe-type or champagne flute-type femurs was reported as < 10% in Noble's original study.[12] Moreover, the percentage is lower for stovepipe-type femurs than for champagne flute-type femurs.[31,32] As a normal distribution of our data could not be assumed because of this small sample size, non-parametric statistical methods were used, increasing the risk of Type 2 error.

In conclusion, our use of patient-specific FEAs provided evidence that large cementless Accolade TMZF stems implanted in stovepipe-shaped femurs can shift the mechanical load distribution distally, after achievement of initial fixation. This distal shift in mechanical load distribution could explain the significant loss in BMD in the medial-proximal area of stovepipe femurs post-operatively. The post-operative change in the mechanical stimuli on bone remodelling predicted from our FE simulations was consistent with BMD changes measured over the first post-operative year. The combination of stovepipe femurs and large-size Accolade TMZF stem, therefore, enhances stress shielding after THA, leading to post-operative bone loss in the proximal femur which can occur even after the establishment of successful initial fixation of the stem.

Supplementary material

Figures showing the Accolade TMZF stem, a mesh model, and loading and restriction conditions for finite element analysis are available with this article at www.bjr.boneandjoint.org.uk

References

1. **McLaughlin JR, Lee KR.** Uncemented total hip arthroplasty using a tapered femoral component in obese patients: an 18-27 year follow-up study. *J Arthroplasty* 2014;29:1365-1368.
2. **Khanuja HS, Vakil JJ, Goddard MS, Mont MA.** Cementless femoral fixation in total hip arthroplasty. *J Bone Joint Surg [Am]* 2011;93-A:500-509.
3. **Pettersen SH, Wik TS, Skallerud B.** Subject specific finite element analysis of implant stability for a cementless femoral stem. *Clin Biomech (Bristol, Avon)* 2009;24:480-487.
4. **White CA, Carsen S, Rasuli K, et al.** High incidence of migration with poor initial fixation of the Accolade stem. *Clin Orthop Relat Res* 2012;470:410-417.
5. **Cooper HJ, Jacob AP, Rodriguez JA.** Distal fixation of proximally coated tapered stems may predispose to a failure of osteointegration. *J Arthroplasty* 2011;26(6 Suppl):78-83.
6. **Bessho M, Ohnishi I, Matsuyama J, et al.** Prediction of strength and strain of the proximal femur by a CT-based finite element method. *J Biomech* 2007;40:1745-1753.
7. **Herrera A, Panisello JJ, Ibarz E, et al.** Long-term study of bone remodelling after femoral stem: a comparison between dexa and finite element simulation. *J Biomech* 2007;40:3615-3625.
8. **Jonkers I, Sauwen N, Lenaerts G, et al.** Relation between subject-specific hip joint loading, stress distribution in the proximal femur and bone mineral density changes after total hip replacement. *J Biomech* 2008;41:3405-3413.
9. **Hirata Y, Inaba Y, Kobayashi N, et al.** Comparison of mechanical stress and change in bone mineral density between two types of femoral implant using finite element analysis. *J Arthroplasty* 2013;28:1731-1735.
10. **Ike H, Inaba Y, Kobayashi N, et al.** Comparison between mechanical stress and bone mineral density in the femur after total hip arthroplasty by using subject-specific finite element analyses. *Comput Methods Biomech Biomed Engin* 2015;18:1056-1065.
11. **Engh CA, Massin P, Suthers KE.** Roentgenographic assessment of the biologic fixation of porous-surfaced femoral components. *Clin Orthop Relat Res* 1990;257:107-128.
12. **Noble PC, Alexander JW, Lindahl LJ, et al.** The anatomic basis of femoral component design. *Clin Orthop Relat Res* 1988;235:148-165.
13. **González Della Valle A, Slullitel G, Piccaluga F, Salvati EA.** The precision and usefulness of preoperative planning for cemented and hybrid primary total hip arthroplasty. *J Arthroplasty* 2005;201:51-58.
14. **Gruen TA, McNeice GM, Amstutz HC.** "Modes of failure" of cemented stem-type femoral components: a radiographic analysis of loosening. *Clin Orthop Relat Res* 1979;141:17-27.
15. **Keyak JH, Rossi SA, Jones KA, Skinner HB.** Prediction of femoral fracture load using automated finite element modeling. *J Biomech* 1998;31:125-133.
16. **Gracia L, Ibarz E, Puértolas S, et al.** Study of bone remodeling of two models of femoral cementless stems by means of DEXA and finite elements. *Biomed Eng Online* 2010;9:22.
17. **Huiskes R, Weinans H, van Rietbergen B.** The relationship between stress shielding and bone resorption around total hip stems and the effects of flexible materials. *Clin Orthop Relat Res* 1992;274:124-134.
18. **Kerner J, Huiskes R, van Lenthe GH, et al.** Correlation between pre-operative periprosthetic bone density and post-operative bone loss in THA can be explained by strain-adaptive remodelling. *J Biomech* 1999;32:695-703.
19. **Herrera A, Panisello JJ, Ibarz E, et al.** Comparison between DEXA and finite element studies in the long-term bone remodeling of an anatomical femoral stem. *J Biomech Eng* 2009;131:041013.
20. **Sapkas GS, Papagelopoulos PJ, Stathakopoulos DP, et al.** Evaluation of lumbar spine bone mineral density in the anteroposterior and lateral projections by dual-energy X-ray absorptiometry. *Orthopedics* 2001;24:959-963.
21. **Lerch M, Kurtz A, Stukenborg-Colsman C, et al.** Bone remodeling after total hip arthroplasty with a short stemmed metaphyseal loading implant: finite element analysis validated by a prospective DEXA investigation. *J Orthop Res* 2012;30:1822-1829.
22. **Engh CA Jr, Young AM, Engh CA Sr, Hopper RH Jr.** Clinical consequences of stress shielding after porous-coated total hip arthroplasty. *Clin Orthop Relat Res* 2003;417:157-163.
23. **McAuley JP, Culpepper WJ, Engh CA.** Total hip arthroplasty. Concerns with extensively porous coated femoral components. *Clin Orthop Relat Res* 1998;355:182-188.
24. **Ruben RB, Fernandes PR, Folgado J.** On the optimal shape of hip implants. *J Biomech* 2012;45:239-246.
25. **Nishino T, Mishima H, Kawamura H, et al.** Follow-up results of 10-12 years after total hip arthroplasty using cementless tapered stem - frequency of severe stress shielding with synergy stem in Japanese patients. *J Arthroplasty* 2013;28:1736-1740.
26. **Engh CA, Bobyn JD, Glassman AH.** Porous-coated hip replacement. The factors governing bone ingrowth, stress shielding, and clinical results. *J Bone Joint Surg [Br]* 1987;69-B:45-55.
27. **Sköldenberg OG, Bodén HSG, Salemyr MOF, Ahl TE, Adolphson PY.** Periprosthetic proximal bone loss after uncemented hip arthroplasty is related to stem size: DXA measurements in 138 patients followed for 2-7 years. *Acta Orthop* 2006;77:386-392.
28. **Draenert KD, Draenert YI, Krauspe R, Bettin D.** Strain adaptive bone remodelling in total joint replacement. *Clin Orthop Relat Res* 2005;430:12-27.
29. **Brown TD, Pedersen DR, Gray ML, Brand RA, Rubin CT.** Toward an identification of mechanical parameters initiating periosteal remodeling: a combined experimental and analytic approach. *J Biomech* 1990;23:893-905.
30. **Skinner HB, Kilgus DJ, Keyak J, et al.** Correlation of computed finite element stresses to bone density after remodeling around cementless femoral implants. *Clin Orthop Relat Res* 1994;305:178-189.
31. **Husmann O, Rubin PJ, Leyvraz PF, de Roguin B, Argenson JN.** Three-dimensional morphology of the proximal femur. *J Arthroplasty* 1997;12:444-450.
32. **Laine HJ, Lehto MU, Moilanen T.** Diversity of proximal femoral medullary canal. *J Arthroplasty* 2000;15:86-92.

Funding Statement
- Y. Inaba declares receiving a research grant from Smith & Nephew Japan K.K. and Stryker Japan K.K.

Author Contribution
- M. Oba: Study design, Data collection, Performing finite element analyses, Manuscript preparation.
- Y. Inaba: Study design, Manuscript preparation, Principal investigator.
- N. Kobayashi: Statistical analysis and interpretation.
- H. Ike: Image data review, Data collection, Performing finite element analyses.
- T. Tezuka: Image data review, Data collection, Performing finite element analyses.
- T. Saito: Study design, Manuscript preparation.

ICMJE conflict of interest
- None declared.